CARDIAC MAGNETIC FIELD MAP TOPOLOGY QUANTIFIED BY KULLBACK-LEIBLER ENTROPY IDENTIFIES PATIENTS WITH HYPERTROPHIC CARDIOMYOPATHY

A. Schirdewan, A. Gapelyuk, R. Fischer, L. Koch, H. Schütt, U. Zacharzowsky
R. Dietz, L. Thierfelder
Medical Faculty of the Charité, Franz-Volhard-Klinik, Helios Klinikum-Berlin, Wiltbergstr. 50, D-13125 Berlin, Germany

N. Wessel
Department of Physics, University of Potsdam, Am Neuen Palais 10, D-14415 Potsdam, Germany

Keywords: Patient screening, Cardiac magnetic field mapping, Kullback-Leibler entropy; Hypertrophic cardiomyopathy.

Abstract: Hypertrophic Cardiomyopathy (HCM) is defined clinically by the growing/thickening of especially the left heart muscle. In up to 70 % of cases, there is a family history of this condition. The individual risk for affected patients strongly varies and depends on the individual manifestation of the disease. Therefore, an early detection of the disease and identification of high-risk subforms is desirable. In this study we investigated the capability of cardiac magnetic field mapping (CMFM) to detect patients suffering from HCM (n=33, 43.8 ± 13 years, 13 women, 20 men; vs. a control group of healthy subjects, n=57, 39.6 ± 8.9 years; 22 women, 35 men; vs. patients with confirmed cardiac hypertrophy due to arterial hypertension, n=42, 49.7 ± 7.9 years, 15 women, 27 men). We introduce for the first time a combined diagnostic approach based on map topology quantification using Kullback-Leibler (KL) entropy and regional magnetic field strength parameters. The cardiac magnetic field was recorded over the anterior chest wall using a multichannel-LT-SQUID system. We show that our diagnostic approach allows not only detecting HCM affected individuals, but also discriminates different forms of the disease. Thus, CMFM including KL entropy based topology quantifications is a suitable tool for HCM screening.

1 INTRODUCTION

Hypertrophic cardiomyopathy (HCM) is a primary inherited cardiac muscle disorder characterized by hypertrophy, usually in the absence of other loading conditions, such as hypertension. In the general population, familial hypertrophic cardiomyopathy (FHCM) is the most common cardiovascular genetic disorder with a prevalence of about 1 in 500 adults. HCM is caused by mutations in several cardiac sarcomeric contractile protein genes. So far mutations in 11 different genes, including the cardiac ß-myosin heavy chain (ß-MHC), myosin-binding protein C (MyBP-C), cardiac troponins T and I, α-tropomyosin, myosin light chains and, more recently, titin and actin genes, have been identified (Seidman 1998, Thierfelder 1994). Histo-pathological hallmarks of HCM are myocyte hypertrophy with disarray and increased cardiac fibrosis, leading to electrical remodeling processes in the myocardium (Maron, 2004). The clinical course of the disease is heterogeneous. Clinical presentation of HCM ranges from minimal or no symptoms to the development of the most serious complications, including atrial fibrillation, heart failure, and sudden death, often at a young age and in the absence of previous symptoms (Spirito, 1989). One of the strongest predictors of disease progression to heart failure and finally death is the existence of a hemodynamic obstruction of the left ventricular outflow tract during systole, which per convention is defined by a pressure gradient ≥30 mmHg measured by continuous wave doppler echocardiography. Therefore, it is of clinical importance to distinguish between the obstructive (HOCM) and non obstructive (HNCM) form of the disease. Familial hypertrophic cardiomyopathy is

Schirdewan A., Gapelyuk A., Fischer R., Koch L., Schütt H., Zacharzowsky U., Dietz R., Thierfelder L. and Wessel N. (2008).
CARDIAC MAGNETIC FIELD MAP TOPOLOGY QUANTIFIED BY KULLBACK-LEIBLER ENTROPY IDENTIFIES PATIENTS WITH HYPERTROPHIC CARDIOMYOPATHY.
In *Proceedings of the First International Conference on Bio-inspired Systems and Signal Processing*, pages 445-452
DOI: 10.5220/0001064504450452

the most common structural cause of sudden cardiac death in individuals aged less than 35 years, especially in competitive athletes. Thus, an early recognition of the disease is useful for risk assessment and starting drug therapy and non-pharmacological treatment options to prevent prognostic fatal heart failure and mortality. The detection of affected patients remains still challenging. Genetic testing allows accurate diagnosis of HCM and its causing mutations, but has some limitations. First, DNA screening is not part of routine clinical evaluation, and identifies the mutation actually only in 50-60 % of patients. Secondly, as shown by DNA genotype-phenotype correlation studies, the disease expression varies not only between unrelated individuals but also within the same family. At present, clinical screening and risk stratification includes medical history, clinical examination, 12-lead ECG at rest and under physical exercise, Holter-ECG, echocardiography and cardiac magnetic resonance imaging. Follow-up examinations should be encouraged in affected patients on a 12-18 month basis. For their first degree relatives annual evaluations are recommended in the adolescence period and every 5 years beyond the age of 18.

Noninvasive electrophysiological diagnosis in patients suffering from HCM is usually done by electrocardiography, rarely by body surface potential mapping studies. However, information content from ECG signals seems to be limited and not disease specific (Maron, 1990). As an alternative to electrocardiography, magnetocardiography can be used for a study of cardiac electrophysiological phenomena, especially myocardial electrical remodeling processes. Changes in myocardial electrical properties were shown to be associated with the development of hypertrophic cardiomyopathy (Fananapazir, 1989). Multi channel cardiac magnetic field mapping (CMFM) reflects the magnetic fields generated by the myocardial electrical currents occurring during the cardiac cycle. CMFM signals have several advantages: (1) they are little influenced by the tissues between skin and heart; (2) they are sensitive to tangential currents that arise in the border zones of cardiac tissue with different electrophysiological properties; (3) they consider the track of electrical vortex currents; and (4) their properties make it possible to accurately localize intracardiac sources (Fenici, 2003).

We therefore investigated the capability of CMFM to detect patients suffering from HCM, including those who have a very mild phenotype or are asymptomatic. The purpose of the study was to develop a CMFM based diagnostic approach to improve screening/diagnosis of HCM. We introduced the calculation of Kullback-Leibler entropy as a parameter to quantify the topology of cardiac magnetic field distribution. We use the term map topology as a synonym for the two-dimensional distribution of cardiac magnetic field strength. Note that this term is therefore independent from field strength amplitudes. The mathematical method, first described by Kullback and Leibler in 1951, provides a value of the similarity between two probability distributions (Kullback).

We further analyzed, whether a combination of KL based topology quantification with regional field strength parameters improves the discrimination power of the automatic diagnostic algorithm.
Our study was done to address three questions:
1. Can CMFM distinguish between HCM individuals and healthy control subjects or patients with cardiac hypertrophy of other causes?
2. Is it possible to discriminate between the two main phenotype subgroups of HCM; patients with (HOCM) and without (HNCM) obstruction of the left ventricular outflow tract?
3. How do CMFM based classification algorithms perform, when prospectively applied for screening in HCM families with known genetic status?

2 METHODS

2.1 Patients

Thirty three patients (HCM, n=33, 43.8 ± 13 years, 13 women, 20 men) affected by hypertrophic cardiomyopathy were recruited from our hospital based cardiomyopathy-outpatient center. The diagnosis was confirmed by complex diagnostic tests including echocardiography and magnetic resonance imaging established on evidence-based guidelines. HCM was diagnosed by the presence of a non-dilated and hypertrophied left ventricle in the absence of another cardiac or systemic disease (e.g. hypertension or aortic stenosis) capable of producing the magnitude of hypertrophy observed. Nineteen patients suffered from the obstructive form and 14 patients from hypertrophic non obstructive cardiomyopathy.

The total number of subjects in the control group (NoHCM) was n=99. We recruited a healthy volunteers group from an occupational health center. The 57 healthy volunteers (age 39.6 ± 8.9 years; 35 men and 22 women) had normal findings in

echocardiography, bicycle ergometry, ECG and Holter-ECG for many years. No control subject had a history of cardiac diseases or symptoms. Forty two patients with essential arterial hypertension (HYP, n=42, 49.7 ± 7.9 years, 15 women and 27 men) were also included in this study, fulfilling the following criteria: known hypertension on pharmacological therapy; echocardiographicly estimated left ventricular hypertrophy (Framingham heart study classification FHC 1-2); no prior clinical manifestation or angiographic documentation of coronary artery disease; no evidence of prior myocardial infarction. The NoHCM group consists of both healthy volunteers and hypertensives (together n=99) to get a more realistic control group for familiar HCM screening.

Two families with genetically proofed HCM (ß-MHC, α-Tropomyosin; 4 HNCM, 1 HOCM, 22 family members in total) were investigated prospectively to check the accuracy of the MFM screening tool.

Our internal review board approved the study and written informed consent was obtained.

2.2 Magnetocardiographic Measurements

The cardiac magnetic field was recorded over the anterior chest wall using a seven channel magnetic measurement system (Cryoton Ltd, Moscow) based on low temperature Superconducting Quantum Interference Device (LT-SQUID), coupled with an axial second order gradiometer (baseline 5.5 cm, pickup coil diameter 2 cm). The component of the magnetic field perpendicular to the chest wall was registered in a 38 point grid (Fig. 1a). To improve the signal to noise ratio all measurements were done in a magnetically shielded room (VAC Akb3b) with a shielded factor better than 10000 at 10 Hz. Typical system performance in this environment was 7 fT in unit band. The measurements were done sequentially at six measurement positions (Fig. 1a) to cover a mapping area of 20x20 cm. Recording time was 30 seconds per point with an acquisition rate of 1000 Hz and a bandwidth of 0.01 – 130 Hz. The ECG lead II was recorded simultaneously as a time reference signal for further processing. Thereafter, signal averaging techniques and offset corrections were applied. Averaged data were then transformed from irregular measurement grid to the regular 6x6 point grid (20 cm width and height) using thin-plate-spline surface. Fig.1b shows averaged cardiac magnetic

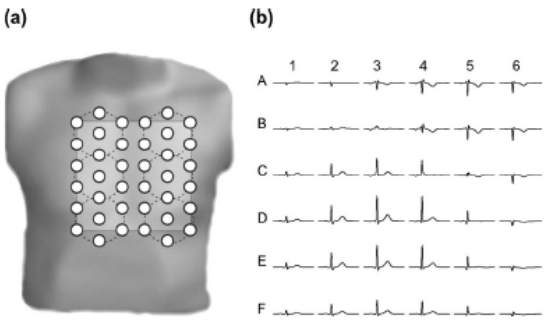

Figure 1: The layout of cardiac magnetic field map (CMFM) measurement: (a) CMFM measurement grid based on a seven channel system. The dashed lines denote six sequential measurement positions. (b) Cardiac magnetic field waveforms transformed into a regular grid (6x6) corresponding to the light grey square in panel (a).

signals for the regular grid. The strength of the cardiac magnetic field was in the range of 10 – 100 pT (picotesla, 10-12 Tesla). The MFM amplitude depends on the distance between measurement plane and patient heart. To compensate this effect we normalized magnetic field strength by the mean absolute value during QRS averaged over 36 points of rectangular grid.

2.3 Cardiac Magnetic Field Map Quantification

After averaging we obtained 1000 samples for each of the 36 measurement positions (Fig 1b), leading to 1000 different CMFM. Thus, the dimensionality of measured data is very high and therefore, we have to reduce it. One solution we present here is based on the concept of Kullback-Leibler entropy to quantify the topology of each map. Suppose that $Q=\{Q_i\}$ (i=1,..,36 – the number of measurement positions; 1: A1, …, 6: A6, 7: B1, …, 12: B6, …36: F6 in Fig 1b) is a given reference well-behaved probability distribution (all $Q_i>0$) and that $P=\{P_i\}$ (i=1,..,36) is some trial probability distribution. The difference of information content of P compared to the reference distribution Q is quantified by the Kullback-Leibler entropy

$$KL(P,Q) = \sum_{i=1}^{36} P_i * \ln \frac{P_i}{Q_i} \quad (1)$$

The Kullback-Leibler (KL) entropy can be considered as a kind of distance between the two probability distributions, though it is not a real distance measure because it is not symmetric. In our study, KL entropy was used to quantify differences in topology between magnetic field maps of a single subject compared with a reference maps. For each

time point, the group mean CMFMs of subjects without HCM was used as a reference map. To quantify topology independent from amplitudes, each CMFM was normalized to get a probability distribution. For maps very similar to the reference we obtain a KL entropy value near zero, differences in topology lead to higher KL entropy values.

For each time point between the onset of QRS and the offset of T-wave, KL values describing differences in topology were calculated. In order to avoid inadequate comparisons due to interindividual differences in QRS and STT duration, we limited the considered time intervals to the shortest QRS and STT lengths in the study population. To identify sub segments with the highest differences in KL values between compared groups, we calculated the discriminant index (DI) for every time point as follows: the absolute differences of mean KL values in both groups were divided by the standard deviation of all cases. Mean KL values during QRS and STT subintervals with a DI value greater than 0.8 were considered as classification parameters KLQRS(DI>0.8) and KLSTT(DI>0.8).

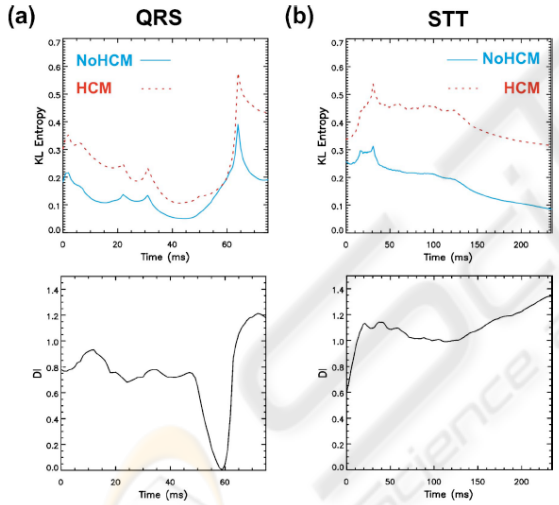

Figure 2: Mean group Kullback-Leibler (KL) entropy values over time during QRS (a) and STT (b). NoHCM group values are denoted with solid (blue) lines and HCM group values with dashed (red) lines (reference maps: NoHCM group). Lower panels give discriminant index (DI) values during QRS (a) and STT (b) intervals respectively: KL values for time intervals where DI was higher than 0.8 (dashed lines) are considered for KLQRS(DI>0.8) and KLSTT(DI>0.8) calculation.

To assess regional differences in magnetic field strength, which cannot be captured by topology, we calculated 36 regional parameters (QRSA1-F6, for positions see Fig. 1b) as mean values of magnetic field strength during QRS complex. Data processing was performed in two steps: classification rules were determined, firstly to discriminate between groups with and without HCM, and secondly to discriminate patients with different forms of HCM. For each step classification performance was tested for KL parameters, regional features and then for their combinations. Finally, the best set of predictors was prospectively applied to identify members of HCM families affected by the disease.

3 RESULTS

Discrimination of HCM Individuals from Healthy Control Subjects and Patients with Cardiac Hypertrophy of other Causes (NoHCM). The mean KL values of the HCM and NoHCM groups during QRS and STT interval are given in Fig. 2 (upper panels), with the corresponding DI values in the lower panels. Only the beginning and parts of the second half of the QRS are discriminating (DI>0.8) for these groups, whereas for STT almost the whole segment is distinctive. These subintervals were used to calculate KLQRS(DI>0.8) and KLSTT(DI>0.8). Mean values of these parameters differed significantly between the two groups (Tab. 1). LDA based on these two features yielded a sensitivity of 78.8 % and specificity of 86.9 % (Tab. 1) with an overall correct classification rate of 84.8 %. Next, we estimated discrimination power of regional parameters based on mean values of magnetic field strength in each grid position. Forward stepwise discriminant analysis was performed to select the best two feature set: QRSB3 and QRSF3. QRSB3 was positive in the NoHCM and negative in the HCM group (Tab. 1, $p < 10\text{-}8$). For QRSF3 mean values of both groups were comparable and not significantly different. However, this parameter was automatically selected by LDA because it provides orthogonal information to QRSB3 to separate both groups. The overall classification rate based on these two regional parameters was lower than with KL based: The specificity of 85.9 % was comparable with KL features but the sensitivity of 66.7 % (cross-validated only 63.6 %) was substantially lower (Tab. 1).

Table 1: Descriptive statistics of patient groups without HCM (NoHCM) and with HCM as well as their separability. Data are given as mean values ± SE and percentage of correctly classified (CC) cases. If 'leave one out' crossvalidated results of discriminant function analysis differ from the original results, they are shown in parentheses. P-values were obtained with the Mann-Whitney-U-test (univariate cases) and the Wilks-Lambda test (linear discriminant function). Three classification approaches were used: (a) KL: based on Kullback-Leibler entropy mean values for QRS and STT time intervals where discriminant index (DI) was higher than 0.8, (b) Regional: based on selected regional parameters, (c) KL+Regional: based on selected KL and regional parameters.

		NoHCM	HCM	P - value
KL	$KL_{QRS(DI>0.8)}$	0.14 ± 0.007	0.27 ± 0.019	$4.8*10^{-10}$
	$KL_{STT(DI>0.8)}$	0.11 ± 0.015	0.33 ± 0.03	$1.1*10^{-10}$
	CC	86.9 %	78.8 %	$3.9*10^{-17}$
Regional	QRS_{B3}	0.45 ± 0.07	-0.59 ± 0.14	$7.8*10^{-9}$
	QRS_{F3}	0.7 ± 0.05	0.68 ± 0.12	0.34
	CC	85.9 %	66.7 % (63.6 %)	$6.2*10^{-12}$
KL+Regional	QRS_{A6}*	-0.46 ± 0.02	-0.37 ± 0.06	0.44
	CC	88.9 %	84.8 %	$6.9*10^{-19}$

As a last step, we combined KL and regional features and applied forward stepwise LDA to find the best set of three parameters. This set included the KL parameters KLQRS(DI>0.8), KLSTT(DI>0.8) and the regional parameter QRSA6. The mean values of the latter parameter again did not significantly differ between both groups, but the combination of these three parameters improved the overall classification rate from 84.8 % to 87.9 % (sensitivity: 84.8 %, specificity: 88.9 %, area under ROC curve: 0.94). The correct classification rates for the subgroups included were 98.2 % in normal subjects, 76.2 % in hypertensive patients, 85.7 % in patients with HNCM and 84.2 % in patients with HOCM.

Discrimination of Obstructive from non Obstructive Forms of HCM. For this analysis, KL entropy was calculated using the averaged maps of the HOCM group as the reference. The mean KL values of HOCM and HNCM groups during QRS and STT interval are given in Fig. 3 (upper panels), with the corresponding DI values in the lower panels. Obviously, the only informative part to separate HOCM from HNCM is the time interval between 57 and 77 ms of the QRS (DI>0.8). Mean values of KLQRS(DI>0.8) differed significantly ($p<10^{-4}$) between both groups (Tab. 2). Using only this parameter, 78.8 % of patients were correctly classified (78.9 % from HOCM group and 78.6 % from HNCM group).

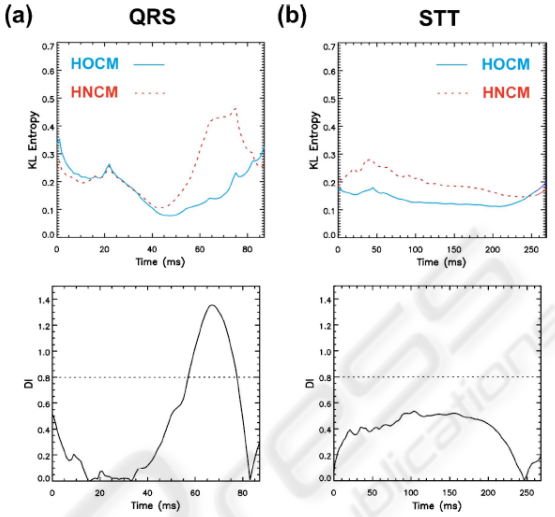

Figure 3: Mean group Kullback-Leibler (KL) entropy values over time during QRS (a) and STT (b). HOCM group values are denoted with solid (blue) lines and HNCM group values with dashed (red) lines (reference maps: HOCM group). Lower panels give discriminant index (DI) values during QRS (a) and STT (b) intervals respectively: KL values for time intervals where DI was higher than 0.8 (dashed lines) are considered for KLQRS(DI>0.8) calculation.

Table 2: Descriptive statistics of patients with HNCM and HOCM as well as their separability. Data are given as mean values ± SE and percentage of correctly classified (CC) cases. If 'leave one out' cross-validated results of discriminant function analysis differ from the original results, they are shown in parentheses. P-values were obtained with the Mann-Whitney-U-test (univariate cases) and the Wilks-Lambda test (linear discriminant function). Three classification approaches were used: (a) KL: based on Kullback-Leibler entropy mean values for QRS where discriminant index (DI) was higher than 0.8, (b) Regional: based on selected regional parameters, (c) KL+Regional: based on selected KL and regional parameters.

		HNCM	HOCM	P - value
KL	$KL_{QRS(DI>0.8)}$	0. 4 ± 0.04	0.16 ± 0.03	$5.1*10^{-5}$
	CC	78.6 %	78.9 %	$3.8*10^{-5}$
Regional	QRS_{F5}	0.67 ± 0.28	2.26 ± 0.34	$2*10^{-3}$
	CC	71.4 %	63.2 %	$1*10^{-3}$
KL+Regional	QRS_{A3}*	-0.73 ± 0.3	-1.31 ± 0.3	0.08
	CC	100 % (92.9 %)	94.7 % (89.5 %)	$1.5*10^{-7}$

Next, we estimated discrimination power of regional parameters, which were calculated for the same time

interval (57-77 ms of QRS). Forward stepwise discriminant analysis found QRSF5 to be the best discriminating parameter (Tab. 2). Overall classification rate using QRSF5 was 66.7 % (63.2 % patients from the HOCM group and 71.4 % from the HNCM group were correctly classified). Again, regional parameters demonstrated a lower classification power.

As the last step, we combined KL and regional parameters and performed a forward stepwise LDA. KLQRS(DI>0.8) and QRSA3 were selected. Overall classification rate for this parameter set was 97 % (94.7 % of HOCM and 100 % of HNCM patients were correctly classified, area under ROC curve: 0.97).

Prospective Screening of Two HCM Families. Application of the two classification algorithms based on the selected sets of combined KL and regional features yielded a correct classification of all 22 family members. This was true not only for detection of HCM affected individuals (5 out of 22 family members), but also for discrimination between different forms of the disease (1 HOCM vs. 4 HNCM).

4 CONCLUSIONS

This study investigated the capability of CMFM to detect patients affected by HCM. The most important findings are, that a KL based topology quantification of cardiac magnetic field distribution discriminates HCM from non HCM and distinguishes between different forms of HCM (HOCM and HNCM), and that a combination with regional field strength parameters improves the discrimination results to a level relevant for clinical application.

Discrimination of HCM Individuals from Healthy Control Subjects and Patients with Cardiac Hypertrophy of other Causes (NoHCM). Both the large variability of the disease expression and the resulting complexity of the CMFM raise difficulties for the magnetophysiologic diagnostic evaluation of HCM. The present paper proposes a new diagnostical approach based on CMFM. Different analysis techniques are currently used for evaluation of cardiac magnetic field maps. This includes for example the estimation of changes in magnetic field orientation through the cardiac cycle and the calculation of QRS-ST-T wave integrals (Van Leeuwen, 2006). We applied for the first time the methodology of Kullback-Leibler entropy for analysis of CMFM to investigate the diagnostic information content in topology related to the status “HCM affected or not”. As we could show, KL values increase with the deviation of map topology compared to the reference field distribution. The idea to use relative entropy measures to classify medical data had already successfully been applied to EEG, HRV and MRI-analyses. Using the KL approach, we found significant differences in map topology during QRS and STT interval between HCM patients and the mixed control group of healthy volunteers and hypertensives. For the process of depolarization the most significant differences were found during the early part (5-20 ms) and within the second half (62-75 ms) of this time period. In contrast, the same was true for nearly the whole repolarization period (STT interval) with marked map topology deviations of the HCM group, revealed by the discriminant index. The analysis of the CMFM using two parameters based on the Kullback-Leibler entropy measures correctly classified 84.8 % of the tested groups. As the control group contained also patients with cardiac hypertrophy due to arterial hypertension, our results strongly suggest that Kullback-Leibler based map quantification revealed specific topological features in HCM patients. They may originate from the pathognomonic ventricular remodeling process, which includes myocardial disarray, left ventricular hypertrophy (LV) and fibrosis. Typically, the LV hypertrophy shows asymmetric distribution with diffuse or segmental pattern of left ventricular wall thickening, most involving the septal region (Saumarez, 1992). This is accompanied by changes in the electrical properties especially at the initial and the last part of QRS, both due to a loss of electrical forces because of transmural myocardial fibrosis and abnormal electrical activation of hypertrophied ventricular septum (Dumont, 2006). Echocardiographic and MRI studies showed that the balance of these electrical forces is primarily a function of the relation of upper anterior septal thickness to right ventricular wall thickness and to upper left ventricular posterior wall thickness. In a non-invasive electrocardiographic imaging study of ventricular activation, Ramanathan et al. (2006) demonstrated an epicardial right ventricular breakthrough in the anterior paraseptal region during the earliest ventricular activation under physiological conditions in healthy volunteers. At the end of the ventricular activation sequence, an apex-to-base activation of the posterior left ventricle was displayed. Based on this description of the

ventricular activation sequence, our findings suggest that within the first 20 ms of the ventricular activation paraseptal parts of the right ventricle could contribute to the observed differences in CMFM topology. In contrast, the map topology differences at the end of the QRS could reflect the influence of regional LV wall hypertrophy and myocardial fibrosis on the electrophysiological myocardial properties, especially if the propagation wave front turns from apical to posterior basal LV. These findings are consistent with those from invasive electrophysiological and morphological LV studies (Schumacher, 2005). Myocardial scarring and its electrophysiological consequences like slowed and fragmented intraventricular conduction also contributed to the specific magneto-physiological HCM phenotype.

Changes in repolarization in HCM patients were also found in ECG studies (Barletta, 2005). The most common abnormalities are related to the ST-segment and the T-wave. This is in consistence with our findings of differences in KL entropy values at the STT interval. They probably emanate from myocardial disarray, fibrosis and small vessel disease leading to scarred myocardium due to regional ischemia (Basso, 2000). HCM does not affect the ventricles uniformly; it is likely that there are areas of diseased myocardium with abnormalities in conduction and refractoriness and heterogeneity of refractoriness, especially related to distal hypertrophy with craniocaudal asymmetry.

Compared with KL measurements, we also found significant regional deviations of magnetic field strengths during depolarization period (QRS), especially in the superior (sensor position B3) and inferior (sensor position F3) part of the mapped area. However, the overall classification rate using only these parameters was lower compared to the KL based set. Specificity was comparable with KL method but sensitivity was substantially lower. A possible explanation for the lower classification rate could be that regional parameters are more sensitive to measurement conditions, especially to the position of the patient's heart relative to the measurement system. Even with a presumed constant distance between sensors and thorax surface, the variations in patients' anatomy result in different heart-sensor distances. Automatic adjustments to solve this problem are under investigation (Burghoff, 2000).

In contrast to the lower efficacy of the mean values of magnetic field strength approach, the classification rate improved adding a regional parameter to the KL features. Since the crossvalidation did not differ from the original results the improvement in classification is due to a higher information content of the combined parameter set.

Discrimination of Obstructive from non Obstructive Forms of HCM. In order to find a discriminant function for separation of HCM subforms (HOCM vs. HNCM), we applied the same approach but now using the HOCM group maps as the reference for KL entropy calculation. As shown by high DI values, KL based topology differed only in a short time interval within the second part of depolarization process (57-77ms). The analysis of regional magnetic field differences revealed that most significant differences between these two HCM subforms exist in the inferior part of the mapped area (sensor position F5). HOCM is characterized by a predominantly septal hypertrophy, which leads to chronic obstruction of the left ventricular outflow tract and consecutively to an increase in wall stress, myocardial ischemia, increased cell death and fibrosis.

Using gadolinium contrast-enhanced MRI, Choudhury et al. found in asymptomatic or mildly symptomatic patients with HCM that the extent of scar increased significantly in relation to wall thickness on a regional basis. The electrophysiological consequences are regional prolongation of the bipolar endocardial potentials and the occurrence of fractionated and split potentials, which directly point to an underlying inhomogeneity of the myocardial excitation with a shift to earlier activation of the lateral LV wall due to septal conduction delay. This probably led to the observed deviation in CMFM map topology between HOCM and HNCM patients in the second part of the QRS interval, which could be quantified by using the KL entropy method. The alterations of regional electrophysiological properties at hypertrophic septal areas are responsible for the observed changes in the inferior mapped area.

Intended to detect HCM subforms, KL entropy measures were superior to the analysis of regional map differences. But, adding a regional parameter QRSA3 to KL entropy parameters, the classification result improved to 97 % with a sensitivity of 100 % for HNCM and a specificity of 94.7 % for HOCM.

Feasibility of the Approach and Conclusions. The correct classification of 5 HOCM and HNCM patients out of 22 family members, in which the diagnosis was confirmed by genetic testing, showed in a prospective part of the study the feasibility of the presented diagnostic algorithm. Our results give

evidence, that KL entropy as a natural distance measure between two probability distributions is an effective tool to obtain discrimination information from CMFM measurements. It is important to point out that the KL tool is applicable to CMFM analysis in a population characterized by a broad spectrum of magnetophysiological and clinical phenotype expression. Prospective screening of HCM family members is strongly recommended, including serial echocardiographic and electrocardiographic examinations (Maron, 2004).

In conclusion, a combined diagnostic algorithm based on KL entropy topology quantification and regional parameters of cardiac magnetic field maps is a suitable tool for HCM screening and discrimination between different forms of the disease.

REFERENCES

Barletta, G., Lazzeri, C., Franchi, F. et al. 2004, Hypertrophic cardiomyopathy: electrical abnormalities detected by the extended-length ECG and their relation to syncope. *Int J Cardiol* 97 (1): 43-8

Basso, C., Thiene, G., Corrado, D. et al. 2000, Hypertrophic cardiomyopathy and sudden death in the young: pathologic evidence of myocardial ischemia. *Hum Pathol* 31 (8): 988-98

Burghoff, M., Nenonen, J., Trahms, L. Katila T. 2000, Conversion of magnetocardiographic recordings between two different multichannel SQUID devices. *IEEE Trans Biomed Eng* 47 (7): 869-75

Dumont, C. A., Monserrat, L., Soler, R., et al. 2006, Interpretation of electrocardiographic abnormalities in hypertrophic cardiomyopathy with cardiac magnetic resonance. *Eur Heart J* 27 (14): 1725-31

Fananapazir, L., Tracy, C. M., Leon, M. B. et al. 1989, Electrophysiologic abnormalities in patients with hypertrophic cardiomyopathy. A consecutive analysis in 155 patients. *Circulation* 80 (5): 1259-68

Fenici, R. , Brisinda, D., Nenonen J., Fenici P. 2003, Phantom validation of multichannel magnetocardiography source localization. *Pacing Clin Electrophysiol* 26 (1 Pt 2): 426-30

Kullback S., Leibler R. A. 1951, On information and sufficiency. *Ann Math Stat* 22 (1): 79-86

Maron B. J. 1990, Q waves in hypertrophic cardiomyopathy: a reassessment. *J Am Coll Cardiol* 16 (2): 375-6

Maron, B. J., McKenna, W. J., Danielson, G. K. et al. 2003, Task Force on Clinical Expert Consensus Documents and the European Society of Cardiology Committee for Practice Guidelines. *J Am Coll Cardiol* 42 (9): 1687-713

Maron, B. J., Seidman J. G., Seidman C. E. 2004. Proposal for contemporary screening strategies in families with hypertrophic cardiomyopathy. *J Am Coll Cardiol* 44 (11): 2125-32

Ramanathan, C., Jia, P., Ghanem, R. et al. 2006, Activation and repolarization of the normal human heart under complete physiological conditions. *Proc Natl Acad Sci U S A* 103 (16): 6309-14

Saumarez, R. C., Camm, A. J. , Panagos, A.. et al. 1992, Ventricular fibrillation in hypertrophic cardiomyopathy is associated with increased fractionation of paced right ventricular electrograms. *Circulation* 86 (2): 467-74

Schumacher, B., Gietzen, F. H., Neuser, H. et al. 2005, Electrophysiological characteristics of septal hypertrophy in patients with hypertrophic obstructive cardiomyopathy and moderate to severe symptoms. *Circulation* 112 (14): 2096-101

Seidman C. E. and Seidman J. G. 1998 Molecular genetic studies of familial hypertrophic cardiomyopathy. *Basic Res Cardiol* 93 Suppl 3 13-6

Spirito, P., Chiarella, F., Carratino, L. et al. 1989, Clinical course and prognosis of hypertrophic cardiomyopathy in an outpatient population. *N Engl J Med* 320 (12): 749-55

Thierfelder, L. , Watkins, H., MacRae, C. et al. 1994 Alpha-tropomyosin and cardiac troponin T mutations cause familial hypertrophic cardiomyopathy: a disease of the sarcomere. *Cell* 77 (5): 701-12

Van Leeuwen, P., Hailer, B., Lange S., Gronemeyer , D. H. 2006, Identification of patients with coronary artery disease using magnetocardiographic signal analysis. *Biomed Tech (Berl)* 51 (2): 83-8